ACS APPLIED MATERIALS & INTERFACES

Research Article

www.acsami.org

Photocurrent Enhancement by Multilayered Porphyrin Sensitizers in a Photoelectrochemical Cell

Peter K. B. Palomaki, Marissa R. Civic, and Peter H. Dinolfo*

Department of Chemistry and Chemical Biology, Rensselaer Polytechnic Institute, 125 Cogswell, 110 Eighth Street, Troy, New York 12180, United States

Supporting Information

ABSTRACT: Multilayer Zn(II) tetraphenylporphyrin chromophores, assembled using copper-catalyzed azide−alkyne cycloaddition (CuAAC), provide a new sensitization scheme that could be useful in dye-sensitized solar cells (DSSCs). We report on the photoelectrochemical responses of multilayer films of Zn(II) 5,10,15,20-tetra(4-ethynylphenyl)porphyrin (**1**) assembled on planar ITO substrates operating as a p-type DSSC using three different redox mediators. The traditional I^-/I_3^- redox couple results in the greatest short circuit current densities (J_{SC}) but very low open circuit potentials (V_{OC}). The use of cobalt sepulchrate ($[Co(sep)]^{2+/3+}$) and cobalt tris-bipyridine ($[Co(bpy)_3]^{2+/3+}$) as redox mediators generates higher V_{OC} values, but at the expense of lower photocurrents. These results highlight the inherent differences in the interactions between the redox mediator and Zn(II) tetraphenylporphyrin multilayer films. Increasing the porphyrin content through multilayer growth proved to be effective in increasing the performance of photoelectrochemical cells with all three redox mediators. Cells using I^-/I_3^- reached maximum performance (power output) at five porphyrin layers, $[Co(bpy)_3]^{2+/3+}$ at five layers, and $[Co(sep)]^{2+/3+}$ at three layers. For all mediators, J_{SC} increases with the addition of porphyrin layers beyond a monolayer. However, J_{SC} reaches a maximum value at a point greater than one layer after which it decreases, presumably due to exciton diffusion limitations and the insulating effects of the multilayer film. Similarly, all cells also reach a maximum V_{OC} beyond one porphyrin layer. We show that porphyrin arrays assembled using newly developed CuAAC layer-by-layer growth may be useful as a multilayer sensitization scheme for use in photoelectrochemical cells.

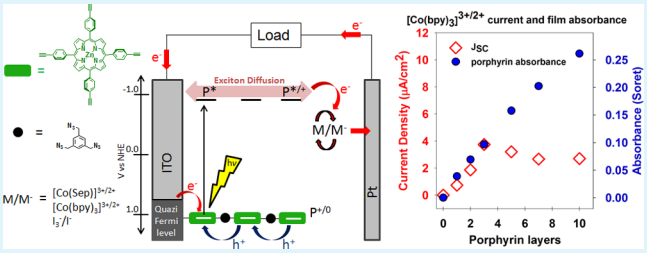

KEYWORDS: *porphyrin, light harvesting, dye-sensitized solar cells, layer-by-layer, multilayer films*

INTRODUCTION

Research concerning the sensitization of semiconductor surfaces with organic- and inorganic-based chromophores has been underway since the late 1960s.[1−3] Attempts to utilize dye-sensitized flat electrodes for solar energy conversion were, for the most part, very inefficient.[4−6] A large increase in overall efficiency was achieved by O'Regan and Grätzel, who developed a high-surface-area nanoporous semiconducting photoanode on which to adsorb sensitizer chromophores.[7] Typically employing a ruthenium polypyridine sensitizer covalently attached to porous nanocrystalline titania and I^-/I_3^- redox shuttle electrolyte, dye-sensitized solar cells (DSSCs) have become a very active research topic in the past two decades.[8−11] Recently, DSSCs using porphyrin sensitizers and cobalt polypyridine based redox mediators have shown great promise with efficiencies rising above 12%.[12,13] Improvements are still needed in order to approach the efficiency of inorganic-based solid-state photovoltaics, but DSSCs offer the distinct advantage of being comprised of relatively inexpensive and solution-processable materials.

One potential method for improving DSSC efficiency involves replacement of the dark cathode electrode (typically platinum) in the n-type DSSC with a p-type DSSC, or photocathode, thus creating a tandem cell.[14] Compared to the Grätzel style n-type DSSCs, p-type photoelectrochemical cells have received significantly less research attention (thousands of references for n-type versus less than ∼25 for p-type).[14] These devices operate in a fashion analogous to n-type DSSCs, but with current flowing in the opposite direction. Unfortunately, the most efficient p-type DSSC created to date displays only a 0.41% efficiency under AM1.5 light conditions, far below that of the best n-type DSSC.[15] Clearly, improvements in p-DSSCs are necessary in order to move closer to the goal of a tandem DSSC.

Despite the advantages of high surface area electrodes in traditional Grätzel cells, flat electrodes provide a more controlled environment on which to study photoelectrochemical phenomena accompanying sensitization and related processes. Additionally, single crystal or polycrystalline thin film electrodes may provide increased performance over defect-ridden nanoporous electrodes by reducing the number of trap sites and imperfections inherent to nanoporous semiconductor

Received: May 21, 2013
Accepted: June 17, 2013
Published: June 17, 2013

   dx.doi.org/10.1021/am401923f | ACS Appl. Mater. Interfaces 2013, 5, 7604−7612

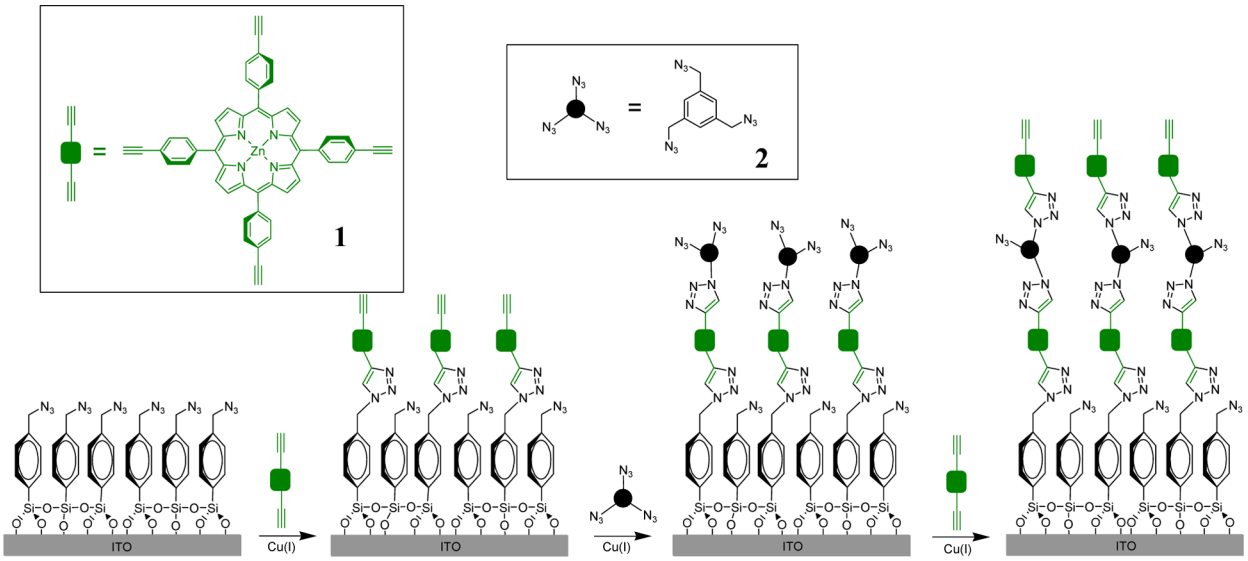

Figure 1. Fabrication of a two-layer porphyrin multilayer film on a benzyl SAM-functionalized ITO substrate.

photoelectrodes.[3] These photoanodes could lead to greater operating potentials and improved current collection if they can be used in conjunction with a high dye loading and/or nanoscale three-dimensional electrode architectures.

In an effort to improve the light absorption and tunability of sensitized electrodes, we have developed a facile method for assembling molecular multilayers on various planar oxide substrates utilizing copper(I)-catalyzed azide−alkyne cycloaddition (CuAAC) or "click" chemistry.[16−18] Figure 1 outlines the method for fabricating porphyrin multilayers via CuAAC on an indium tin oxide (ITO) electrode. First, a clean ITO slide is functionalized with an azide-terminated self-assembled monolayer (SAM). We have chosen the aromatic SAM, 4-(trimethoxysilyl)benzyl azide, in an effort to minimize the insulating effects of traditional alkane-based SAMs and promote higher conductivity between the electrode and porphyrin film. Once the ITO is functionalized with an azide-terminated SAM, Zn(II) 5,10,15,20-tetra(4-ethynylphenyl)porphyrin (**1**) is reacted with the SAM in the presence of a Cu(I) catalyst to generate 1,4-substituted 1,2,3-triazole linkages. Next, an additional CuAAC reaction is performed with a linker molecule, such as 1,3,5-tris(azidomethyl)benzene (**2**), to regenerate the azide rich surface. This two-step process is repeated until the desired number of porphyrin layers is achieved. This multilayer fabrication process is rapid, uses an inexpensive coupling catalyst, and is amenable to a wide range of molecules functionalized with either azides or alkynes. Porphyrins were chosen for this study because of their high molar absorptivity at the Soret peak and our previous success in building high quality multilayer films with **1**.[16−18] We believe that this multilayer fabrication methodology could also be employed for the functionalization of nanoscale three-dimensional electrode architectures.[19−21]

There are numerous examples of porphyrins employed as sensitizers for photoelectrochemical cells;[10,12,22,23] however, there are only a limited number of examples where multilayered porphyrins are used to improve photogalvanic performance.[24−26] In two of these examples the photoelectrochemical cells generate cathodic current on ITO and gold electrodes (i.e., p-type DSSC behavior).[24,25] In the other example, a sacrificial electron donor (triethanolamine) is used to aid in the generation of anodic photocurrent.[26] In the case of p-type DSSC operation, photocurrent is achieved via excited state oxidative quenching of the porphyrin followed by hole-hopping through the multilayer film to the electrode. Based on these previous examples, we expect that our multilayers will exhibit similar cathodic photocurrents (p-DSSC behavior) in the presence of a suitable redox mediator when assembled on ITO. It should be noted that others have been successful in improving photocurrent output and device performance via the incorporation of non-porphyrin multilayered sensitizers.[27,28]

Herein we will explore the usefulness of porphyrin multilayers assembled via CuAAC in a photoelectrochemical cell operating in a p-type fashion. We characterize the performance of the cells via current density−potential (J−V) curves, photocurrent action spectra, and photocurrent transients with three different redox mediators. Many redox mediators have been explored for use in DSSCs,[10] but by far the most commonly used redox mediators today are cobalt$^{II/III}$ polypyridine complexes and I^-/I_3^-. We use cobalt sepulchrate ($[Co(sep)]^{2+/3+}$), cobalt tris-bipyridine ($[Co(bpy)_3]^{2+/3+}$), and I^-/I_3^- as three structurally and electrochemically diverse redox mediators (Scheme 1).

RESULTS AND DISCUSSION

Absorbance of Multilayer Porphyrin Films. We have demonstrated previously that multilayered porphyrin films can be grown reproducibly using CuAAC on a variety of substrates.[16−18,29] Figure 2 shows the absorbance profile of

Scheme 1

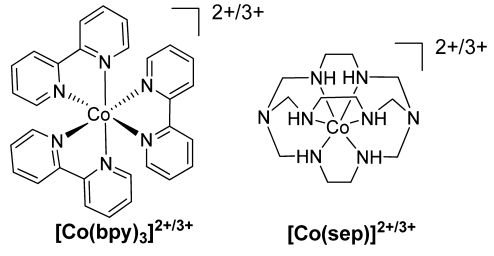

dx.doi.org/10.1021/am401923f | ACS Appl. Mater. Interfaces 2013, 5, 7604−7612

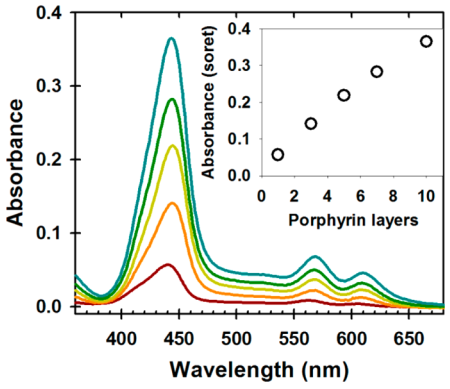

Figure 2. Absorbance profile for porphyrin multilayer films grown using CuAAC on ITO with 1, 3, 5, 7, and 10 porphyrin layers. Inset shows the absorbance at the Soret max for the same films.

films grown as outlined in Figure 1. The intensities of the porphyrin Soret peak and Q-bands increase linearly with number of layers (26 milli-absorbance units (mAU) per layer at the Soret maximum near 440 nm, 4.4 mAU/layer at 566 nm, and 2.8 mAU/layer at 608 nm). Films grown in this manner show a broadened absorbance profile compared to the solution absorbance due to J-aggregation effects between closely packed porphyrins.[16]

Redox Mediator Selection. For this study, we selected the redox couples $[Co(bpy)_3]^{2+/3+}$, $[Co(sep)]^{2+/3+}$, and I^-/I_3^- for our photoelectrochemical system. Although I^-/I_3^- has been used extensively in DSSC devices, several drawbacks are associated with this redox shuttle including its corrosive nature and large driving force needed for efficient regeneration of the ground state sensitizer.[7,30] $[Co(bpy)_3]^{2+/3+}$ and similar analogs have been used in numerous DSSCs recently due to their stable and noncorrosive properties as well as their ability to achieve larger open circuit potentials (V_{OC}) and greater efficiencies than I^-/I_3^-.[12,13,31,32] $[Co(bpy)_3]^{2+/3+}$-based mediators have also been used in p-type and tandem DSSCs.[33,34] $[Co(sep)]^{2+/3+}$ provides an alternative cobalt-based redox mediator for p-type DSSCs with a more negative reduction potential than $[Co(bpy)_3]^{2+/3+}$ (−0.32 V for $[Co(sep)]^{2+/3+}$ vs 0.30 V for $[Co(bpy)_3]^{2+/3+}$). $[Co(sep)]^{2+/3+}$ provides an interesting comparison of how the reduction potential of the redox mediator affects the performance of the cell. Additionally, cobalt mediators are an attractive system because of their slow self-exchange kinetics resulting from their high internal reorganization energy that accompanies the spin flip from low spin Co(III) to high spin Co(II).[35] Figure 3 shows the midpoint potentials of the three redox mediators used in this study along with the proposed operational mechanism of our photoelectrochemical cell in aqueous electrolyte. It is worth noting porphyrin multilayer films on ITO have previously been shown to operate as p-type DSSCs using I^-/I_3^-.[24]

We have electrochemically determined the potential of $[Co(sep)]^{2+/3+}$ to be −0.32 V vs NHE and $[Co(bpy)_3]^{2+/3+}$ to be 0.30 V vs NHE in 0.1 M KCl (aq) when using a platinum working electrode (see the Supporting Information, Figures S1 and S2). Numerous processes are possible for the reduction of I_3^- for the I^-/I_3^- redox mediator, thus it is difficult to assign an exact potential; however, we have applied three important potentials from the literature to reactions that contribute primarily to its properties as a redox mediator.[30] Since these photoelectrochemical cells operate in a p-type fashion, I_3^- is most likely the active electron acceptor. Due to the complexity and multielectron nature of the $I_3^- + 2e^- \rightarrow 3I^-$ redox transition, it is unlikely that this reaction is responsible for the excited state quenching of porphyrin multilayer. Rather, the single electron reduction of I_3^- ($I_3^- + e^- \rightarrow I_2^{\cdot-} + I^-$) at 0.04 V vs NHE is the more likely quenching process.[36] This redox potential is significantly more negative than the midpoint potential for I^-/I_3^- (0.54 V).

The maximum theoretical V_{OC} of the p-type photoelectrochemical cell is determined by the difference between the potential of the ITO working electrode and the midpoint potential of the redox mediator $E(M/M^-)$. The potential of the ITO electrode can be initially approximated by the first porphyrin oxidation for **1** in a multilayer film ($E(P/P^+)$ = 1.02 V vs NHE).[16] Table 1 lists the maximum theoretical V_{OC} for

Table 1. Midpoint Potentials of the Redox Mediators, Theoretical Maximum Achievable V_{OC}, and ΔG_{CT} from the Porphyrin Excited State ($^1P^*$) to the Redox Mediator (M)[a]

	redox couple			
	I_3^-/I^-	$I_3^-/I_2^{\cdot-}$	$[Co(bpy)_3]^{3+/2+}$	$Co(sep)^{3+/2+}$
midpoint potential	0.54	0.04	0.30	−0.32
maximum V_{OC} (V)	0.48	0.98	0.72	1.36
ΔG_{CT}	−1.58	−1.08	−1.33	−0.72

[a]All potentials are reported vs. NHE in aqueous solution.

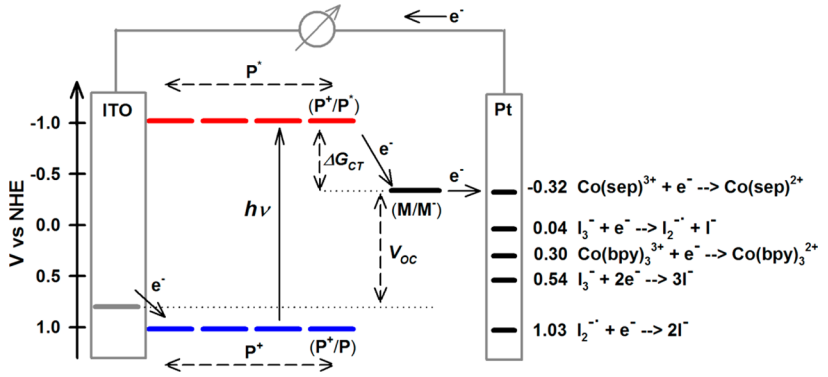

Figure 3. Diagram of the proposed multilayer photocurrent generation mechanism as well as the potentials of redox mediators used in this study. Redox potentials for $[Co(sep)]^{2+/3+}$ and $[Co(bpy)_3]^{2+/3+}$ in aqueous solution and porphyrin **1** were experimentally determined. Potentials for the I^-/I_3^- redox couple in aqueous solution are taken from literature.[30]

the redox mediators used in this study and the free energy for charge transfer (ΔG_{CT}) from the porphyrin singlet excited state ($^1P^*$) to the redox mediator (M), calculated using eq 1.[37,38]

$$\Delta G_{CT} = E(P/P^+) - E(M/M^-) - E(^1P^*) - e^2/\varepsilon D \quad (1)$$

$E(^1P^*)$ was determined from the intersection of normalized absorption and emission spectra of a monolayer of **1** on silica glass (see Figure S3 in the Supporting Information).[16] Finally, in the last term of eq 1, e is the charge of an electron, ε is the dielectric constant of the solvent, and D is the separation distance between the donor and acceptor estimated from molecular models.

Photocurrent Action Spectra and Quantum Efficiency. Figure 4 shows photocurrent action spectra along with the absorbance profile for five bilayers of **1** and **2** on ITO with all redox mediators. The photocurrent action spectra clearly match the absorbance profile of **1** showing that the porphyrin is responsible for light absorption and current generation. Results are displayed as incident photon to current efficiencies (IPCE = number of electrons generated in external circuit/number of incident photons). The best IPCE achieved for all cells is 1.8% (Table 2) at the porphyrin Soret maximum using I^-/I_3^- at three bilayers of **1** and **2** on ITO. Part of the reason for the low IPCE values is that the films are assembled on a planar ITO substrate and collect only about 30% of the incident light (at the Soret maximum) with 3 bilayers of **1** and **2**. The planar electrode results in a much lower surface area than nanoporous electrodes but allows us to eliminate the complexity of the nanoporous layer and focus on the characteristics of the porphyrin multilayer films. A more meaningful result in this case is the absorbed photon to current efficiency (APCE = number of electrons generated in external circuit/number photons absorbed). This accounts for the portion of light that is being absorbed by the film. When the results are displayed as APCE, a different trend occurs (Table 2). The largest APCE (14.8%) results from using the I^-/I_3^- mediator with two layers of **1**. An APCE of 0.37% was found with two layers of **1** for $[Co(sep)]^{2+/3+}$ and 2.6% for $[Co(bpy)_3]^{2+/3+}$ at seven layers of **1**. It is obvious that although the portion of light absorbed continues to increase with the number of porphyrin layers, the resulting photocurrent does not continue to increase at the same rate.

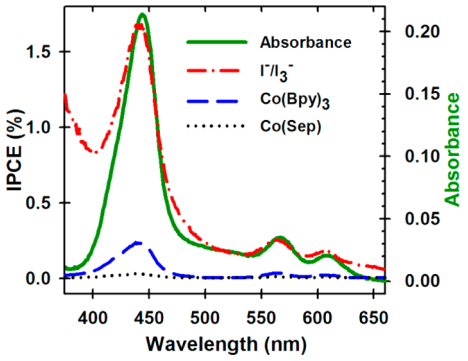

Figure 4. Absorbance profile of five bilayers of **1** and **2** on ITO (green solid line) and photocurrent action spectrum of the same multilayer in photoelectrochemical cells containing different redox mediators.

Photocurrent Transients. Photocurrent transients of 5 bilayers of **1** and **2** on ITO with the three different redox mediators are shown in Figure 5 when illuminated with white light (100 mW/cm^2). The magnitudes of the steady-state short-circuit photocurrents are consistent with the IPCE and APCE values shown above with I^-/I_3^- displaying the highest, followed by $[Co(bpy)_3]^{2+/3+}$ and $[Co(sep)]^{2+/3+}$. The significant difference in photocurrent for I^-/I_3^- versus the cobalt complexes is likely the result of improved charge transfer efficiency (porphyrin excited state quenching), as well as differences in diffusion coefficients for the various redox mediators (vide infra).[33,39,40]

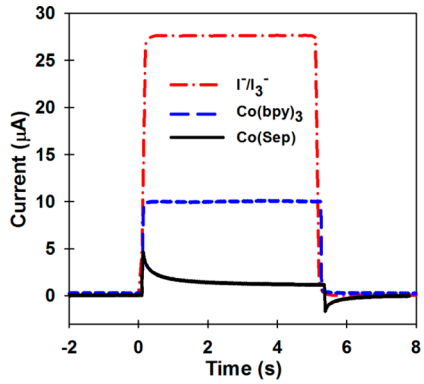

Figure 5. White light photocurrent transients resulting from illumination of a five layer porphyrin sample with $[Co(bpy)_3]^{2+/3+}$, $[Co(sep)]^{2+/3+}$, and I^-/I_3^- electrolytes. The light was turned on at t = 0 s and off at 5 s.

Current–Potential Curves. A selection of J–V curves resulting from white light illumination (100 mW/cm^2) of the multilayer-based photoelectrochemical cells with three redox mediator are shown in Figure 6. A summary of the resulting data can be found in Table S1 in the Supporting Information. Both the short-circuit photocurrent and power conversion efficiency increase beyond a monolayer, reaching a maximum between 3 and 5 bilayers of **1** and **2** on ITO for all three redox mediators. While the values for J_{SC} and V_{OC} tend to vary with number of porphyrin layers, and therefore vary the shape of the curves, the fill factors (FF) for each mediator remain fairly

Table 2. Summary of IPCE and APCE Results for All Redox Mediators at the Porphyrin Soret Maximum (442 nm)

	IPCE (%)			APCE (%)		
porphyrin layers	$[Co(sep)]^{2+/3+}$	$[Co(bpy)_3]^{2+/3+}$	I^-/I_3^-	$[Co(sep)]^{2+/3+}$	$[Co(bpy)_3]^{2+/3+}$	I^-/I_3^-
1	0.02	0.13	0.8	0.32	1.4	7.3
2	0.04	0.29	1.3	0.37	2.3	14.8
3	0.05	0.57	1.8	0.21	2.5	8.0
5	0.04	0.52	1.7	0.18	1.4	5.8
7	0.03	0.37	1.3	0.16	2.6	2.7
10	0.04	0.30	1.1	0.11	1.7	6.3

dx.doi.org/10.1021/am401923f | ACS Appl. Mater. Interfaces 2013, 5, 7604–7612

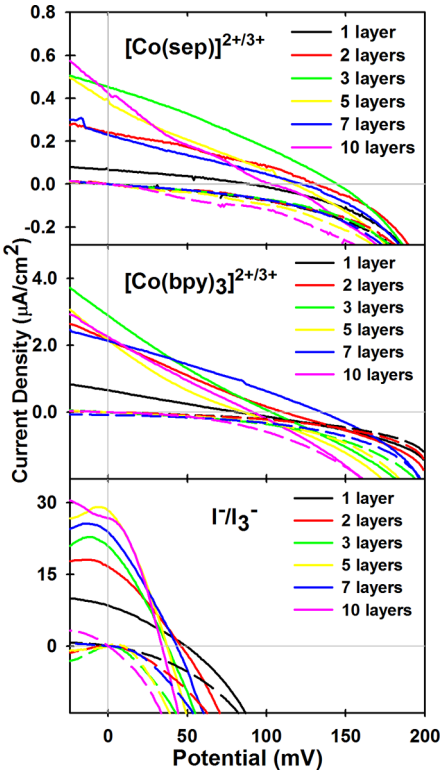

Figure 6. *J*–*V* curves for photoelectrochemical cells containing $[Co(sep)]^{2+/3+}$ (top), $[Co(bpy)_3]^{2+/3+}$ (middle), and I^-/I_3^- (bottom) electrolyte with 1 (black), 2 (red), 3 (green), 5 (yellow), 7 (blue), and 10 (pink) bilayers of **1** and **2** on ITO. Solid lines represent photocurrent from white light illumination (100 mW/cm^2) and dashed lines are dark currents.

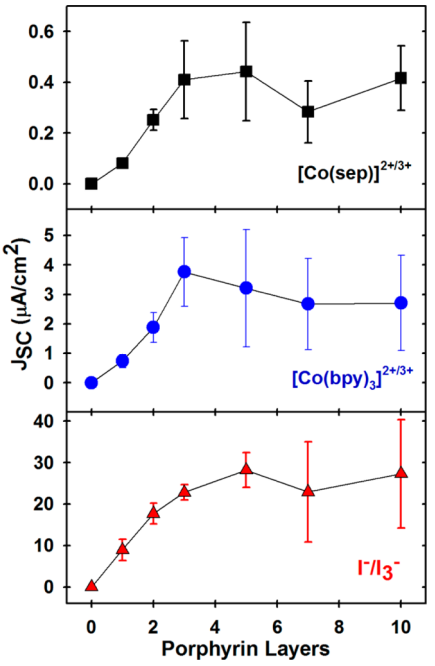

Figure 7. J_{SC} versus number of porphyrin layers for photoelectrochemical cells containing $[Co(sep)]^{2+/3+}$ (black squares), $[Co(bpy)_3]^{2+/3+}$ (blue circles), and I^-/I_3^- (red triangles).

constant averaging 27, 27, and 32% for $[Co(sep)]^{2+/3+}$, $[Co(bpy)_3]^{2+/3+}$, and I^-/I_3^-, respectively. The best overall power conversion efficiency was obtained for cells using I^-/I_3^- with 5 layers of porphyrin resulting in an efficiency of 3.8×10^{-4}%. The highest efficiency obtained with $[Co(sep)]^{2+/3+}$ was 1.4×10^{-5}% with 3 layers and 1.6×10^{-5}% for $[Co(bpy)_3]^{2+/3+}$ with 5 layers of porphyrin. It is important to keep in mind that these films are assembled on planar ITO substrates and only absorb a small fraction of the incident light, so a low overall efficiency is not unexpected.

Figure 7 shows the average values of J_{SC} obtained from *J*–*V* curves for all the devices tested in this study. $[Co(sep)]^{2+/3+}$ achieved a maximum J_{SC} of 0.47 μA/cm^2 at 10 porphyrin layers, whereas $[Co(bpy)_3]^{2+/3+}$ achieves a maximum J_{SC} of 3.8 μA/cm^2 at 3 porphyrin layers. Cells using I^-/I_3^- redox mediator achieved the highest J_{SC} of all three mediators at the largest number of layers (32.8 μA/cm^2 at 10 porphyrin layers). It is interesting to note that the J_{SC} of all three mediators increased with the addition of more porphyrin layers beyond a monolayer but ultimately plateau or decrease slightly. This shows that the use of multilayered light harvesting arrays could be beneficial to improving photocurrent generation and in turn DSSC performance. It is clear that the optimal number of layers is dependent on the redox mediator used and will need to be determined experimentally in order to optimize photoelectrochemical cells utilizing multilayered sensitizers.

The significant difference in J_{SC} for I^-/I_3^- versus the cobalt complexes highlights the variation of charge transfer yield from the excited dye to the redox mediators. The driving force for $^1P^* \rightarrow M/M^-$ charge transfer (ΔG_{CT}) was calculated according to eq 1 and varies depending on the midpoint potential for each mediator (see Table 1). Assuming oxidative quenching of the porphyrin excited state remains in the Marcus normal region[41] for these redox mediators, the observed photocurrent matches the trend in increasing ΔG_{CT} for $[Co(sep)]^{3+}$ to $[Co(bpy)_3]^{3+}$. On the other hand, I_3^-/I^-, which shows the highest photocurrent, has an intermediate value of ΔG_{CT} (−1.08 eV) for the single electron reduction ($I_3^- + e^- \rightarrow I_2^{\cdot-} + I^-$), thus suggesting that ΔG_{CT} is not the sole determining factor of J_{SC}. Variation in rates for back electron transfer from the reduced mediator to the oxidized porphyrin, or underlying ITO electrode, may also play a role in the observed differences in J_{SC}. Given the inner-sphere electron transfer mechanism for I^-/I_3^-, this back electron transfer process should be slow compared to the outer-sphere based cobalt complexes. In the latter case, the blocking layer properties of the multilayers should limit the back electron transfer rates to ITO by creating an insulating film on the electrode surface. This is supported by the increase in J_{SC}, as well as V_{OC} (vide infra), for the first three layers for both $[Co(sep)]^{2+/3+}$ and $[Co(bpy)_3]^{2+/3+}$.

The large difference in photocurrent for I_3^-/I^- versus the other mediators is likely the result of I_3^- forming a preassociation complex with the porphyrin, allowing for efficient oxidative quenching of the porphyrin excited state.[24] Not only is the interaction with the porphyrin different for the mediators, we suspect that I_3^- may be able to penetrate the multilayer film better than the cobalt mediators due to size considerations. This may help explain why the maximum J_{SC} for I^-/I_3^- is observed when 7 porphyrin layers are used, while the maximum J_{SC} is observed at layers 3 and 5 for $[Co(bpy)_3]^{2+/3+}$ and $[Co(sep)]^{2+/3+}$, respectively. In an effort to examine the permeability of the porphyrin multilayers toward I^-/I_3^-, multilayer films comprised of 5, 7, and 10 bilayers of **1** and **2** on ITO were soaked in electrolyte solutions of I^-/I_3^-. Difference spectra comparing the multilayer films before and

after soaking revealed a new absorbance peak at 374 nm that closely matches the absorbance spectrum of I_3^- (see Figure S4 in the Supporting Information).[42] The new band appeared after only 15 min of soaking and remained fairly constant for up to two hours. A ratio of 1.2−1.9 for $[I_3^-]$:[**1**] was found by comparing the absorption band intensities and molar absorptivies of I_3^- to that of **1**.[42] This suggests there is a significant amount of I_3^- penetrating the multilayer films and is consistent with the higher J_{SC} achieved with this redox mediator.

The observed V_{OC} values for all devices tested in this study are shown in Figure 8. The addition of multilayered

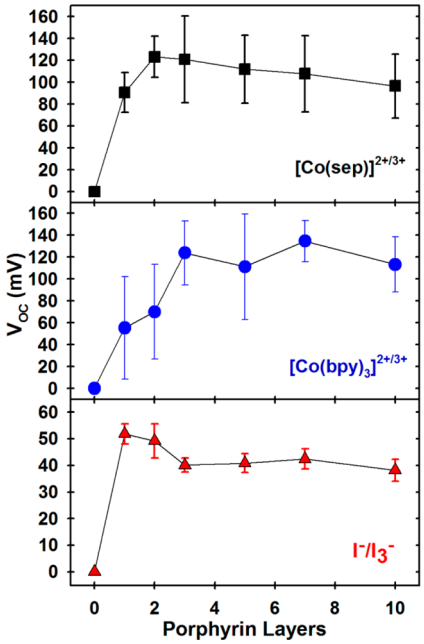

Figure 8. V_{OC} versus number of porphyrin layers for photoelectrochemical cells containing $[Co(sep)]^{2+/3+}$ (black squares), $[Co(bpy)_3]^{2+/3+}$ (blue circles), and I^-/I_3^- (red triangles).

chromophores improved the V_{OC} performance, but this time for only the cobalt-based redox mediators. $[Co(sep)]^{2+/3+}$ and $[Co(bpy)_3]^{2+/3+}$ displayed the largest V_{OC} at approximately 120 mV after 3 layers and remained somewhat constant up to 10 layers. Photoelectrochemical cells using I^-/I_3^- redox mediator achieved a maximum V_{OC} of 52 mV after only one porphyrin layer and decreased thereafter with additional porphyrin layers. The low V_{OC} for I^-/I_3^- suggests that disproportionation of $I_2^{\cdot-}$ to I_3^- and I^-, which is rapid in aqueous solution,[43,44] may be affecting the midpoint potential of the mediator at the counter electrode as the bulk electrolyte will be comprised primarily of I_3^- and I^-.

The experimentally observed V_{OC} for all three mediators are significantly less than the theoretical values. The porphyrin sensitized ITO electrode employed in these studies utilizes a benzyl-siloxane SAM as the connection between the ITO surface and multilayer film. The insulating nature of this self-assembled monolayer results in a potential drop across this interface to the redox active porphyrins, which manifests itself as a deviation from ideal electrochemistry and an apparent shift in the formal oxidation potential.[45] Additionally the porphyrin multilayer may also act as an insulating layer in its neutral form, adding a second potential drop across the electrode−multilayer interface. These interfacial potential distributions are expected to shift the potential of the ITO electrode to more negative values, thus lowering the theoretical V_{OC}.

Photocurrent Generation Mechanism. As expected, the cells used in this study display a cathodic photocurrent upon illumination. It has been seen before that porous multilayer porphyrin films operate as p-type DSSCs in the presence of the I^-/I_3^- redox couple.[24] Results suggest that the mechanism of photocurrent generation in these types of cells occurs through oxidative quenching of the porphyrin excited state ($^1P^*$) by the redox mediator; thus, the interaction of the oxidized redox mediator with the porphyrins controls the yield and rate of charge separation and therefore photocurrent. In the case of I^-/I_3^-, the I_3^- forms a preassociation complex with the porphyrin which results in rapid oxidative quenching of $^1P^*$ by I_3^-.[24] It appears that the cobalt mediators function in a manner similar to I^-/I_3^- (sans the preassociation complex). We presume the excited porphyrin is able to reduce Co(III) to Co(II) based on the more negative porphyrin excited state reduction potential compared to that of the redox mediators. After oxidation of the porphyrin by Co(III) or I_3^-, a hole-hopping transfer mechanism occurs where the hole travels to the electrode through the porphyrin layers, where it recombines with an electron from the external circuit to regenerate a neutral porphyrin. To the best of our knowledge, this report demonstrates the use of cobalt-based redox mediators in a multilayered porphyrin sensitized film for the first time.

We have established that multilayer porphyrin films grown using CuAAC are nonporous and effectively block penetration of $[Co(bpy)_3]^{2+/3+}$ after only a few layers.[16] If a porphyrin below the surface of the multilayer is protected from the mediator, the excited porphyrin may not be able to interact directly with the redox mediator to undergo oxidative quenching. For multilayered films to increase sensitization, one of two events must occur. Either the redox mediator would need to efficiently diffuse in and out of the porphyrin multilayer, or the exciton generated below the surface must migrate to the peripheral of the film in order to interact with the mediator. Because we know the films effectively block $[Co(bpy)_3]^{2+/3+}$, we can safely assume that $[Co(sep)]^{2+/3+}$ will be blocked as well and that exciton diffusion will need to occur in order to realize increases in photocurrent in multilayered porphyrin devices. Upon excitation of a porphyrin within the film (not at the surface) exciton diffusion must take place in order to generate an excited porphyrin near the film−solution interface. This helps to explain the fact that the maximum current does not scale linearly with increased porphyrin content. If a porphyrin deep within the film is excited (Figure 3), exciton migration would need to occur until the exciton reaches the outer surface of the multilayer film where it is able to undergo oxidation by the redox mediator. Following oxidation, the same hole-hopping mechanism as described above would deliver the hole to the ITO surface. Exciton diffusion in our films is most likely random because there is no built-in field or preferred motion for the exciton to proceed. It appears that exciton diffusion becomes a limiting factor to increasing photocurrent at sufficiently thick films. We previously established a thickness of 1.87 nm/bilayers for films of the same molecular components.[18] Exciton diffusion up to tens of nanometers at room temperature has been observed previously in porphyrin thin films.[46,47] It can be seen from Figure 7 that photocurrent reaches a limit around 3−5 porphyrin layers for cobalt(II/III) mediators, suggesting that

dx.doi.org/10.1021/am401923f | ACS Appl. Mater. Interfaces 2013, 5, 7604−7612

exciton diffusion in our films is sufficient to reach the film interface when films are up to 6−9 nm thick.

The size of the redox mediator, and therefore its ability to penetrate the film, may also be related to exciton diffusion and performance. When I^-/I_3^- is used as a redox mediator (the smallest of the three mediators used in this study) it is most likely able to penetrate the multilayer film more easily than either of the two cobalt mediators. This allows the I_3^- acceptor to be in close proximity to more of the porphyrins in the film resulting in a device that does not depend on exciton diffusion reaching the outer porphyrin layer to result in charge separation. With I^-/I_3^- dispersed throughout the film (even at lower layers) the exciton diffusion length may not be the limiting factor in photocurrent generation because charge separation can occur throughout the film. When cobalt mediators are used (much larger than I^-/I_3^- therefore film penetration is limited) exciton diffusion plays a more important role in device performance because charge separation must occur near the film/solution interface.

In addition to exciton diffusion, hole transfer may contribute to limiting photocurrent generation. The hole-hopping mechanism described above will work until the film becomes sufficiently resistive to preclude holes from reaching the ITO electrode. Since the dielectric constant of our films is probably low, hole transfer may become a limiting factor in photocurrent generation.

Lindsey and co-workers have previously studied energy transfer and electronic communication in multiporphyrin arrays.[48−50] These multiporphyrin arrays are generally coupled through diarylethyne linker and are studied in solution phase. They show that there is generally good communication between porphyrins along a linear wire and achieve energy transfer efficiencies of greater than 99% for some molecular wires and energy transfer rates in the 10s of picoseconds time regime.[48] Additionally, they found that hole-hopping occurs readily in multiporphyrin arrays. While our films are structurally different than those mentioned here, they provide a good base for comparison. The lifetime of a Zn-tetraphenyl porphyrin excited state is in the range of 1.49−2.35 ns depending on the solvent.[51,52] This relatively short lifetime may become a limiting factor in photocurrent generation because it may compete with the time it takes for cobalt mediators to oxidize the excited porphyrins. We have begun our study of LbL light harvesting arrays with Zn-porphyrin, but intend to expand our studies to other chromophores in the future.

CONCLUSION

We have shown that p-type DSSCs with redox mediators $[Co(sep)]^{2+/3+}$, $[Co(bpy)_3]^{2+/3+}$, and I^-/I_3^- benefit from a multilayered porphyrin sensitizer film. To the best of our knowledge, this is the first use of $[Co(sep)]^{2+/3+}$ as a redox mediator for any DSSC. Given its high reduction potential, this may be a beneficial redox mediator for p-DSSCs. The highest current densities were achieved with I^-/I_3^- as the redox mediator and the highest potentials were achieved with $[Co(sep)]^{2+/3+}$, as expected from the redox potentials of the three mediators. Maximum power was achieved with a device containing three porphyrin layers and $[Co(bpy)_3]^{2+/3+}$ electrolyte which resulted in an efficiency of 1.5×10^{-3} %. It is important to note that these cells were created on flat electrode surfaces, not high surface area semiconductor electrodes that are more commonly used in DSSCs. Therefore, the low efficiencies are expected because of the low overall absorptivity of the multilayer films. It appears that the limiting factors in performance (after poor light absorption) may be exciton diffusion length as well as the decreased conductivity of the film with increasing thickness. We do not believe that either of the cobalt mediators penetrates the multilayer film substantially or interacts specifically with the Zn-porphyrin. I^-/I_3^- may benefit from being smaller in size (therefore being able to penetrate the film) and having a larger diffusion constant as well as forming a preassociation complex with Zn-porphyrin. For these reasons, cells made with I^-/I_3^- show larger photocurrents than cells made with the cobalt mediators. There may be some benefit to using the larger cobalt mediators in that the porphyrin film will act as a self-passivating layer, preventing the mediator from interacting with the electrode surface. We are in the process of exploring this unique effect of our multilayer films.

The use of CuAAC to build molecular multilayers of porphyrin allows for rapid fabrication of multilayer films, as well as the ability to tune the molecular layers within the film. We plan to investigate other chromophores and molecular components in the CuAAC grown films as well as alternative redox mediators to determine their effect on performance and to optimize photoelectrochemical response. Our first attempt at using CuAAC grown porphyrin multilayer films shows that the films could potentially be used as sensitizers in DSSCs.

EXPERIMENTAL SECTION

Materials. Solvents, ACS reagent grade or better, were purchased from Sigma Aldrich or Fisher Scientific and used as received. Sodium ascorbate (Aldrich) was used as received. Zn(II) 5,10,15,20-tetra(4-ethynylphenyl)porphyrin,[53] tris-(benzyltriazolylmethyl)amine (TBTA),[54] 1,3,5-tris(azidomethyl)benzene,[55] and cobalt sepulchrate trichloride ($[Co(sep)]^{2+/3+}$)[56−58] were synthesized according to literature methods. ITO-coated glass slides were purchased from Delta Technologies (polished float glass, ITO coated one surface, sheet resistance, R_s = 4−8 Ω).

4-(Trimethoxysilyl)benzyl Azide. 4-(Trimethoxysilyl)benzyl azide was synthesized following a previous method[59] with minor modifications. Briefly, 4-(trimethoxysilyl)benzyl chloride was refluxed in acetonitrile with excess sodium azide overnight. The resulting mixture was filtered through a glass frit and the solvent evaporated under reduced pressure to a light yellow liquid that was then filtered through glass wool. ^1H and ^{13}C NMR of the product was consistent with literature values.[59]

Tris-(2,2′-bipyridine)cobalt(III) Chloride ($[Co(bpy)_3]Cl_3$). A slight excess of 2,2′-bipyridine was added to 1 g of $CoSO_4$ dissolved in deionized water with stirring. The complex was then oxidized by adding 30% H_2O_2 dropwise until no additional color change was observed. A saturated aqueous solution of KPF_6 was then added to precipitate $[Co(bpy)_3](PF_6)_3$ which was collected by filtration and washed with additional deionized water. The counteranion was then metathesized to chloride by dissolving the complex in acetone and adding a slight excess of *tetra*-n-butylammonium chloride. $[Co(bpy)_3]Cl_3$ was collected by filtration and washed with additional acetone. ^1H NMR for $[Co(bpy)_3](PF_6)_3$ shows expected peaks (CD_3CN): 8.68 d (6H, J = 7.5 Hz), 8.47 t (6H, J = 8 Hz), 7.73 t (6H, J = 6 Hz), 7.26 d (6H, J = 6 Hz). Cyclic voltammogram of $[Co(bpy)_3]Cl_3$ shows expected one electron reversible wave at 0.098 V vs Ag/AgCl/3 M KCl in 0.1 M KCl at a Pt working electrode (see the Supporting Information).

Electronic Absorbance Spectroscopy. Electronic spectra were taken on a Perkin-Elmer Lambda 950 spectrometer using a solid sample holder. The sample was positioned normal to the incident light. A background spectrum of a SAM functionalized ITO slide was subtracted from each spectrum.

Azido-SAM Formation on ITO. Prior to use, ITO coated glass slides were sonicated in a dilute solution of Alconox, washed with water, acetone, dichloromethane, ethanol, and last DI water, then

submersed in concentrated sulfuric acid for about 30 min. The slides were then rinsed with copious amounts of DI water, dried under a stream of nitrogen, and placed in a Schlenk flask at a pressure of 0.1 mTorr to remove residual water. The slides were submerged in a solution of approximately 1 mM 4-(trimethoxysilyl)benzyl azide in anhydrous toluene. The reaction vessel was then heated at 60−70 °C overnight. After cooling to room temperature the slides were removed and sonicated in toluene for 5 min then washed with acetone, dichloromethane, ethanol, and water, and finally dried in a stream of nitrogen. Slides were placed in an oven at 75 °C for 3 h.

Multilayer Fabrication. *Ethynyl-Porphyrin Layers.* A solution of DMSO, containing <2% water, consisting of 1.3 mM Zn-porphyrin, 0.33 mM CuSO4, 0.36 mM TBTA, and 0.48 mM sodium ascorbate was placed in contact with one side of a SAM-functionalized ITO sample. After 6 min the slide was washed with acetone, dichloromethane, ethanol, and water.

Azidolinker Layer. DMSO solution, containing <8% water, was used as described above consisting of 2.2 mM of 1,3,5-tris-(azidomethyl)benzene, 4.4 mM $CuSO_4$, 4.8 mM TBTA, and 8.9 mM sodium ascorbate. After every linker layer the slide was rinsed for 10−20 s with a solution of 1 mM EDTA to assist in removing copper from the film. Additionally, at the end of the growth of every sample (terminated in porphyrin), the slide was again treated with EDTA as described above.

Platinum/ITO Counter Electrode. ITO slides were cleaned with solvents, dried under a stream of nitrogen, cleaned using a Bioforce Nanosciences UV/Ozone cleaner for about 10 min, and then submersed in a solution of 2.0 mM K_2PtCl_4 in 0.1 M K_2HPO_4. A cyclic voltammogram experiment was run with an Ag/AgCl reference electrode and Pt mesh counter electrode from 0.2 V to −0.5 V vs Ag/AgCl at a scan rate of 50 mV/s for 80 segments (40 cyclic scans). The resulting slides appear gray compared to unplatinized ITO. The K_2PtCl_4 deposition solution was stored in a freezer and reused multiple times with no observed degradation.

Photoelectrochemical Cell Fabrication. Photocurrent measurements were performed in a 2 electrode set up. Multilayers on ITO were used as the working electrode and electrochemically platinized ITO slides were used as the counter electrode. Kapton tape was applied to the counter electrode with a rectangular opening of 1 × 2 cm. Thirty uL of aqueous 0.15 M $[Co(bpy)_3]Cl_3$, 0.15 M $[Co(sep)]Cl_3$, or I^-/I_3^- (0.5 M NaI and 0.01 M I_2) was placed on the counter electrode, then the working electrode was placed multilayer-face down on the counter electrode. The two electrodes were held together using small binder clips with electrolyte filling the space between electrodes. The distance between the two electrodes was determined by using a Perkin-Elmer Lambda 950 scanning UV−vis. An interference fringe pattern was observed in the region between 800 and 2000 nm, which was used to calculate the spacing of the ITO/Pt counter electrode and a glass microscope slide with air in between.[60,61] This cell served as an estimate of the spacing of the photoelectrochemical cell filled with electrolyte. The spacing was determined for seven cells resulting in an average spacing of 63.8 μm with a standard deviation of 0.4 μm.

Photoelectrochemical Measurements. A Horiba Jobin Yvon Fluorolog 3 spectrofluorimeter equipped with a 450 W Xe lamp and dual monochromator was used as the light source for all photocurrent measurements. The photoelectrochemical cell was illuminated from the porphyrin functionalized slide first. All experiments were done with either white light at 2 nm slit width with a glass filter (ca. 2.2 mm) placed in between the light beam and sample to block UV light (at 2 nm slit width total power = 200 mW which resulted in a power density of 100 mW/cm^2) or at single wavelengths with 5 nm slit width. No corrections were made for reflectance from the Pt/ITO counter electrode. A calibrated Si-diode photodetector from Thor Laboratories (model S120VC) and power meter (PMD100USB) were used to account for the output profile of the lamp and monochromators. A Scientech thermal power meter was used to determine the total output power of the white light. Photocurrent action spectra were taken with a 5 nm slit width, 0.1 nm step, and integration time of 0.1 s. Potentials were controlled using a CH Instruments 1222B potentiostat with the counter and reference electrodes connected to the Pt/ITO counter electrode of the photoelectrochemical cell to act as a two electrode system. Photocurrent action spectra and photocurrent transients were acquired with the multilayer working electrode held at 0 V vs the Pt counter electrode. $J-V$ curves were acquired at a scan rate of 50 mV/s. A minimum of three multilayer samples were prepared for each set of $J-V$ curves to obtain the average values of J_{SC}, V_{OC}, FF, and conversion efficiencies.

Electrochemical Measurements. Electrochemical measurements were performed on a CH Instruments 440A potentiostat. Cyclic voltammograms of redox mediators were performed at a concentration of 1 mM in 0.1 M KCl with a Pt disc working electrode, Ag/AgCl/3 M KCl reference electrode, and Pt counter electrode. Solutions were degassed with nitrogen prior to use. Electrochemical determination of the porphyrin oxidation potential as a multilayer film on ITO was taken from our previous studies.[16]

■ ASSOCIATED CONTENT

Ⓢ Supporting Information

Cyclic voltammograms of $[Co(sep)]Cl_3$ and $[Co(bpy)_3]Cl_3$, absorbance and fluorescence spectra of a monolayer of **1** on glass, difference absorbance spectra of multilayers following immersion in I^-/I_3^- electrolyte, and tablet data from $J-V$ curves of multilayer photoelectrochemical measurements. This material is available free of charge via the Internet at http://pubs.acs.org.

■ AUTHOR INFORMATION

Corresponding Author

*E-mail: dinolp@rpi.edu.

Notes

The authors declare no competing financial interest.

■ ACKNOWLEDGMENTS

The authors acknowledge Michael Topka for the fluorescence spectra of porphyrin **1** on glass. This material is based on work supported by Rensselaer Polytechnic Institute and the National Science Foundation under DGE-0333314 and CHE-1255100.

■ REFERENCES

(1) Gerische, H.; Tributsc, H. *Bunsen-Ges. Phys. Chem., Ber.* **1968**, *72*, 437−445.
(2) Tributsc, H.; Gerische, H. *Bunsen-Ges. Phys. Chem., Ber.* **1969**, *73*, 251−260.
(3) Spitler, M. T.; Parkinson, B. A. *Acc. Chem. Res.* **2009**, *42*, 2017−2029.
(4) Alonso, N.; Beley, V. M.; Chariter, P.; Ern, V. *Rev. Phys. Appl.* **1981**, *16*, 5−5.
(5) Matsumura, M.; Nomura, Y.; Tsubomura, H. *Bull. Chem. Soc. Jpn.* **1977**, *50*, 2533−2533.
(6) Willig, F.; Eichberger, R.; Sundaresan, N. S.; Parkinson, B. A. *J. Am. Chem. Soc.* **1990**, *112*, 2702−2707.
(7) O'Reagan, B.; Gratzel, M. *Nature* **1991**, *353*, 737−740.
(8) Hagfeldt, A.; Gratzel, M. *Acc. Chem. Res.* **2000**, *33*, 269−277.
(9) Hagfeldt, A.; Gratzel, M. *Chem. Rev.* **1995**, *95*, 49−68.
(10) Hagfeldt, A.; Boschloo, G.; Sun, L.; Kloo, L.; Pettersson, H. *Chem. Rev.* **2010**, *110*, 6595−6663.
(11) Gratzel, M. *Inorg. Chem.* **2005**, *44*, 6841−6851.
(12) Yella, A.; Lee, H.-W.; Tsao, H. N.; Yi, C.; Chandiran, A. K.; Nazeeruddin, M. K.; Diau, E. W.-G.; Yeh, C.-Y.; Zakeeruddin, S. M.; Gratzel, M. *Science* **2011**, *334*, 629−634.
(13) Yum, J.-H.; Baranoff, E.; Kessler, F.; Moehl, T.; Ahmad, S.; Bessho, T.; Marchioro, A.; Ghadiri, E.; Moser, J.-E.; Yi, C.; Nazeeruddin, M. K.; Grätzel, M. *Nat. Commun.* **2011**, *3*, 631.
(14) Odobel, F.; Le Pleux, L.; Pellegrin, Y.; Blart, E. *Acc. Chem. Res.* **2010**, *43*, 1063−1071.

(15) Morandeira, A.; Fortage, J.; Edvinsson, T.; Le Pleux, L.; Blart, E.; Boschloo, G.; Hagfeldt, A.; Hammarstrom, L.; Odobel, F. *J. Phys. Chem. C* **2008**, *112*, 1721−1728.
(16) Palomaki, P. K. B.; Dinolfo, P. H. *Langmuir* **2010**, *26*, 9677−9685.
(17) Palomaki, P. K. B.; Dinolfo, P. H. *ACS Appl. Mater. Interfaces* **2011**, *3*, 4703−4713.
(18) Palomaki, P. K. B.; Krawicz, A.; Dinolfo, P. H. *Langmuir* **2011**, *27*, 4613−4622.
(19) Kumar, A.; Madaria, A. R.; Zhou, C. *J. Phys. Chem. C* **2010**, *114*, 7787−7792.
(20) Lee, J.-C.; Kim, T. G.; Lee, W.; Han, S.-H.; Sung, Y.-M. *Cryst. Growth Des.* **2009**, *9*, 4519−4523.
(21) Lei, B.-X.; Liao, J.-Y.; Zhang, R.; Wang, J.; Su, C.-Y.; Kuang, D.-B. *J. Phys. Chem. C* **2010**, *114*, 15228−15233.
(22) Campbell, W. M.; Jolley, K. W.; Wagner, P.; Wagner, K.; Walsh, P. J.; Gordon, K. C.; Schmidt-Mende, L.; Nazeeruddin, M. K.; Wang, Q.; Grätzel, M.; Officer, D. L. *J. Phys. Chem. C* **2007**, *111*, 11760−11762.
(23) Waltera, M. G.; Rudineb, A. B.; Wamser, C. C. *J. Porphyrins Phthalocyanines* **2010**, *14*, 759−792.
(24) Splan, K. E.; Massari, A. M.; Hupp, J. T. *J. Phys. Chem. B* **2004**, *108*, 4111−4115.
(25) Abdelrazzaq, F. B.; Kwong, R. C.; Thompson, M. E. *J. Am. Chem. Soc.* **2002**, *124*, 4796−4803.
(26) Hasobe, T.; Imahori, H.; Hiroko, Y.; Sato, T.; Ohkubo, K.; Fukuzumi, S. *Nano Lett.* **2003**, *3*, 409−412.
(27) Byrd, H.; Suponeva, E. P.; Bocarsly, A. B.; Thompson, M. E. *Nature* **1996**, *380*, 610−612.
(28) Sereno, L.; Silber, J. J.; Otero, L.; Bohorquez, M. d. V.; Moore, A. L.; Moore, T. A.; Gust, D. *J. Phys. Chem.* **1996**, *100*, 814−821.
(29) Krawicz, A.; Palazzo, J.; Wang, G.-C.; Dinolfo, P. H. *RSC Adv.* **2012**, *2*, 7513−7522.
(30) Boschloo, G.; Hagfeldt, A. *Acc. Chem. Res.* **2009**, *42*, 1819−1826.
(31) Sapp, S. A.; Elliott, C. M.; Contado, C.; Caramori, S.; Bignozzi, C. A. *J. Am. Chem. Soc.* **2002**, *124*, 11215−11222.
(32) Feldt, S. M.; Wang, G.; Boschloo, G.; Hagfeldt, A. *J. Phys. Chem. C* **2011**, *115*, 21500−21507.
(33) Gibson, E. A.; Smeigh, A. L.; Pleux, L. c. L.; Hammarström, L.; Odobel, F.; Boschloo, G.; Hagfeldt, A. *J. Phys. Chem. C* **2011**, *115*, 9772−9779.
(34) Gibson, E. A.; Smeigh, A. L.; Pleux, L. L.; Fortage, J.; Boschloo, G.; Blart, E.; Pellegrin, Y.; Odobel, F.; Hagfeldt, A.; Hammarström, L. *Angew. Chem., Int. Ed.* **2009**, *48*, 4402−4405.
(35) Hamann, T. W. *Dalton Trans.* **2012**, *41*, 3111−3115.
(36) Gibson, E. A.; Le Pleux, L. c.; Fortage, J. r. m.; Pellegrin, Y.; Blart, E.; Odobel, F.; Hagfeldt, A.; Boschloo, G. *Langmuir* **2012**, *28*, 6485−6493.
(37) Rehm, D.; Weller, A. *Isr. J. Chem.* **1970**, *8*, 259−271.
(38) Rehm, D.; Weller, A. *Ber. Bunsenges. Phys. Chem.* **1969**, *73*, 834−839.
(39) Nelson, J. J.; Amick, T. J.; Elliott, C. M. *J. Phys. Chem. C* **2008**, *112*, 18255−18263.
(40) Feldt, S. M.; Gibson, E. A.; Gabrielsson, E.; Sun, L.; Boschloo, G.; Hagfeldt, A. *J. Am. Chem. Soc.* **2010**, *132*, 16714−16724.
(41) Marcus, R. A.; Sutin, N. *Biochim. Biophys. Acta* **1985**, *811*, 265−322.
(42) Awtrey, A. D.; Connick, R. E. *J. Am. Chem. Soc.* **1951**, *73*, 1842−1843.
(43) Grossweiner, L. I.; Matheson, M. S. *J. Phys. Chem.* **1957**, *61*, 1089−1095.
(44) Rowley, J.; Meyer, G. J. *J. Phys. Chem. C* **2009**, *113*, 18444−18447.
(45) Smith, C. P.; White, H. S. *Anal. Chem.* **1992**, *64*, 2398−2405.
(46) Huijser, A.; Savenije, T. J.; Meskers, S. C. J.; Vermeulen, M. J. W.; Siebbeles, L. D. A. *J. Am. Chem. Soc.* **2008**, *130*, 12496−12500.
(47) Donker, H.; Hoek, A. v.; Schaik, W. v.; Koehorst, R. B. M.; Yatskou, M. M.; Schaafsma, T. J. *J. Phys. Chem. B* **2005**, *109*, 17038−17046.
(48) Holten, D.; Bocian, D. F.; Lindsey, J. S. *Acc. Chem. Res.* **2002**, *35*, 57−69.
(49) Hasselman, G. M.; Watson, D. F.; Stromberg, J. R.; Bocian, D. F.; Holten, D.; Lindsey, J. S.; Meyer, G. J. *J. Phys. Chem. B* **2006**, *110*, 25430−25440.
(50) Ambroise, A.; Kirmaier, C.; Wagner, R. W.; Loewe, R. S.; Bocian, D. F.; Holten, D.; Lindsey, J. S. *J. Org. Chem.* **2002**, *67*, 3811−3826.
(51) Liu, X.; Tripathy, U.; Bhosale, S. V.; Langford, S. J.; Steer, R. P. *J. Phys. Chem. A* **2008**, *112*, 8986−8998.
(52) Karolczak, J.; Kowalska, D.; Lukaszewicz, A.; Maciejewski, A.; Steer, R. P. *J. Phys. Chem. A* **2004**, *108*, 4570−4575.
(53) Onitsuka, K.; Kitajima, H.; Fujimoto, M.; Iuchi, A.; Takei, F.; Takahashi, S. *Chem. Commun.* **2002**, 2576−2577.
(54) Chan, T. R.; Hilgraf, R.; Sharpless, K. B.; Fokin, V. V. *Org. Lett.* **2004**, *6*, 2853−2855.
(55) Song, Y.; Kohlmeir, E. K.; Meade, T. J. *J. Am. Chem. Soc.* **2008**, *130*, 6662−6663.
(56) Gahan, L. R.; Healy, P. C.; Patch, G. J. *J. Chem. Educ.* **1989**, *66*, 445.
(57) Harrowfield, J. M.; Herlt, A. J.; Sargeson, A. M. In *Inorganic Syntheses*; Busch, D. H., Ed.; John Wiley & Sons: New York, 1980; Vol. *20*, op 85−86.
(58) Work, J. B.; McReynolds, J. P. In *Inorganic Syntheses*; Fernelius, W. C., Ed.; John Wiley & Sons: New York, 1946; Vol. *2*, pp 221−222.
(59) Azam, M. S.; Fenwick, S. L.; Gibbs-Davis, J. M. *Langmuir* **2010**, *27*, 741−750.
(60) Karki, L.; Hupp, J. T. *Inorg. Chem.* **1997**, *36*, 3318−3321.
(61) Shin, Y.-g. K.; Brunschwig, B. S.; Creutz, C.; Sutin, N. *J. Phys. Chem.* **1996**, *100*, 8157−8169.